DOI: 10.1002/chem.201001665

# Fullerene–Coumarin Dyad as a Selective Metal Receptor: Synthesis, Photophysical Properties, Electrochemistry and Ion Binding Studies

**Georgia Pagona,[a] Solon P. Economopoulos,[a] George K. Tsikalas,[b] Haralambos E. Katerinopoulos,[b] and Nikos Tagmatarchis*[a]**

**Abstract:** A coumarin derivative with a malonate unit has been synthesized and used for the preparation of a fullerene–coumarin dyad through the Bingel cyclopropanation method. The newly synthesized dyad is soluble in organic solvents and has been fully characterized with traditional spectroscopic techniques. Electronic interactions between the two components of the dyad were probed with the aid of UV/Vis spectroscopy, fluorescence emission, and electrochemistry measurements. Our studies clearly show the presence of electronic interactions between $C_{60}$ and modified coumarin in the ground state; efficient electron-transfer quenching of the singlet excited state of the coumarin moiety by the appended fullerene sphere was also observed. Time-resolved fluorescence measurements revealed lifetimes for the coumarin–$C_{60}$ dyad at a maximum of 50 ps, while the quantum yield was reaching unity. Additionally, the redox potentials of the $C_{60}$–coumarin dyad were determined and the energetics of the electron-transfer processes were evaluated. Finally, after alkaline treatment of $C_{60}$–coumarin, which resulted in the deprotection of carboxylate units, the dyad was tested as a metal receptor for divalent metal cations; ion competition studies and fluorescence experiments showed binding selectivity for lead ions.

**Keywords:** coumarin · dyes/pigments · fullerenes · hybrid materials · metal receptors

## Introduction

Fullerenes provide an interesting platform for designing novel materials with diverse functions. However, direct application of intact fullerenes in devices is limited due to poor solubility, particularly in polar solvents. Among the different approaches explored to overcome the solubility issue is organic functionalization. Developments in the organic modification of fullerenes led to the construction of advanced materials incorporating photo- and/or electroactive units, thus forming novel donor–acceptor dyads,[1] in which fullerene acts as an electron acceptor due to its relatively low reduction potential, extended π-electron system, and low reorganization energy.[2] In view of exploring practical applications, such hybrid fullerene-based materials are considered as key components in molecular electronic,[3] optoelectronic,[4] photonic,[5] and sensor[6] devices, to name a few.

Organic dyes, such as coumarin derivatives, are attractive molecules due to their extended spectral range, high emission quantum yields, and photostability.[7] Moreover, coumarin derivatives are frequently encountered as receptors and signaling units in sensors and biosensors[8] as well as in advanced photophysical systems.[9] Coumarin-based ion indicators generally do not have large extinction coefficients in comparison with the more common fluorescein- and rhodamine-based fluorescent ion indicators. However, the fluorescence intensity per dye molecule is proportional to the product of epsilon and the quantum yield. The respective values of coumarin-based dyes allow for ion detection at low indicator concentrations. Additionally, coumarin indicators can be introduced to cells either by microinjection or as membrane permeable derivatives without causing cell death. The fact that aminocoumarins undergo photoinduced charge transfer upon excitation has been exploited in the design and synthesis of ratiometric fluorescent ion indicators exhibiting blue- or redshifts in their spectra upon ion binding.

[a] Dr. G. Pagona, Dr. S. P. Economopoulos, Dr. N. Tagmatarchis
Theoretical and Physical Chemistry Institute
National Hellenic Research Foundation
48 Vassileos Constantinou Avenue
11635 Athens (Greece)
Fax: (+30) 210-7273794
E-mail: tagmatar@eie.gr

[b] Dr. G. K. Tsikalas, Prof. H. E. Katerinopoulos
Department of Chemistry, University of Crete
71003, Heraklion (Greece)

Supporting information for this article is available on the WWW under http://dx.doi.org/10.1002/chem.201001665.

   

The shift depends on the interaction of the ion with the aminocoumarin donor or acceptor moiety, respectively.[7]

In principle, in fullerene–coumarin dyads not only the characteristic intrinsic properties of the individual components, namely, fullerene and coumarin, would be integrated, but also intriguing behavior, function, and properties, based on intermutual interactions between the individual units, may arise. With only a couple of related reports published from a single group, fullerene–coumarin dyads remained almost unexplored.[10] In this light, herein, we initially focused on the synthesis and characterization of a $C_{60}$–coumarin dyad. Then, optical measurements, in terms of steady-state electronic absorption and fluorescence emission spectroscopy, as well as time-resolved fluorescence emission, combined with electrochemistry, were performed and allowed us to gain insight in electron-transfer processes within the fullerene–coumarin dyad. Finally, the newly prepared dyad was tested for ion-binding ability and found to be selective for lead.

## Results and Discussion

**Synthesis**: The methodology employed for the preparation of the targeted $C_{60}$–coumarin hybrid material is based on the well-established protocol of the Bingel cyclopropanation reaction.[11,12] To this end, coumarin derivative **8** with a malonate unit was synthesized according to the procedure given in Scheme 1. Briefly, 4-(benzyloxy)-2-nitrophenol (**1**)[13] was alkylated under typical Williamson conditions with 1-[(2-bromoethoxy)methyl]benzene to generate 4-(benzyloxy)-1-[2-(benzyloxy)ethoxy]-2-nitrobenzene (**2**) in 92% yield. Then, catalytic hydrogenation of **2** resulted in the formation of aniline derivative **3**, which was subsequently alkylated with methyl bromoacetate (2 equiv) to give compound **4** in 32% yield. Vilsmayer formylation of **4**, followed by deprotection of the benzyl moieties under catalytic conditions led to the formation of salicylaldehyde **6** in 73% yield. Knoevenagel-type reaction allowed the incorporation of the benzothiazol chromophore unit as an extension of the π-conjugated system of the coumarin skeleton, thus giving derivative **7**. The synthesis of methyl 2-benzothiazolyl acetate, as the active component for the Knoevenagel-type reaction, was accomplished through the reaction of zinc acetate dihydrate and *o*-aminothiophenol followed by treatment with malonylchloride monomethyl ester.[14] Eventually, the malonate–coumarin derivative **8** was obtained by treatment of **7** with methyl malonyl chloride. The structure of **8**, as well as all synthetic intermediates, was confirmed by standard analytical and spectroscopic techniques (see the Supporting Information). The formation of the ring system and the malonate side chain in **8** was verified by the $^1$H NMR signals of the vinyl proton at $\delta = 8.96$ ppm and the malonyl unit protons at $\delta = 3.76$ and 3.48 ppm. Additionally, the two signals at $\delta = 166.3$ and 166.7 ppm in the $^{13}$C NMR spectrum verified the presence of the malonyl moiety carbonyls. The MALDI-TOF mass spectrum, in the positive mode, shows a signal at $m/z$ 598.12, corresponding to the molecular ion $[M^+]$ of **8**.

With **8** in hand, we then turned our attention to covalently link it with the fullerene sphere. We followed the literature procedure of the Bingel cyclopropanation,[11,12] in which α-halomalonates were generated in situ by direct treatment with carbon tetrabromide in the presence of 1,8-diazabicyclo[5.4.0]undec-7-ene (DBU) as a base and then reacted with $C_{60}$. To this end, derivative **8** (1 equiv), carbon tetrabromide (1.15 equiv), and DBU (1.35 equiv) were added to a solution of $C_{60}$ (1.3 equiv) in toluene. After stir-

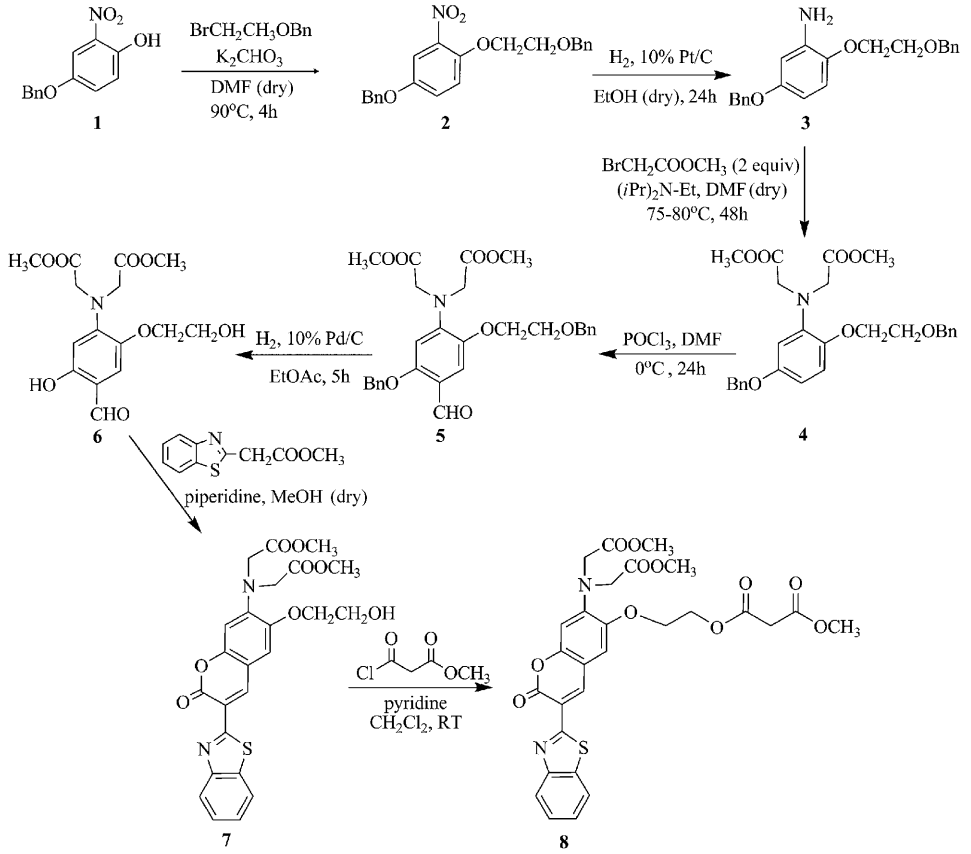


Scheme 1. Synthetic route of **8**. Bn = benzyl.

  

ring at 25 °C for 24 h, the corresponding fullerene–coumarin dyad **9** was isolated in moderate yield (19 %), according to Scheme 2. The structure of **9** was confirmed by $^1$H NMR

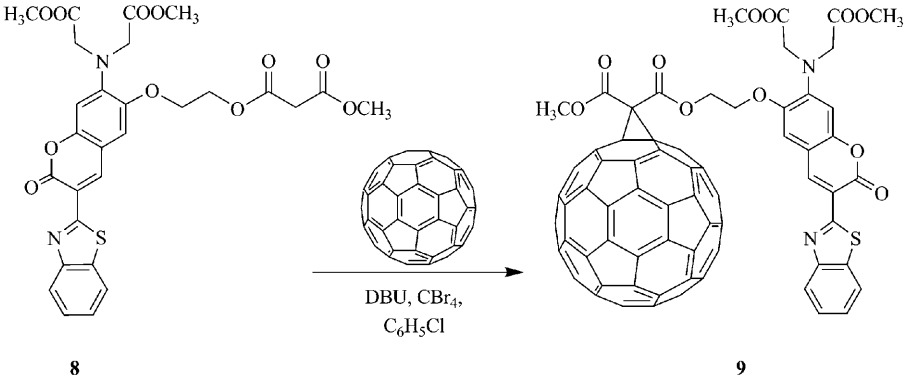


**8** **9**

Scheme 2. Synthesis of **9**.

spectroscopy and MALDI-TOF mass spectrometry. The $^1$H NMR spectrum of **9** is similar to that of **8**, with some of the signals shifted downfield due to the deshielding effect of the fullerene core. The mass of **9** was found by MALDI-TOF mass spectrometry (negative mode) to be *m*/*z* 1317.16, a value that corresponds to the molecular ion of $[M^+]$, thus unambiguously verifying the successful formation of **9**.

Figure 1 shows typical differential scanning calorimetry (DSC) thermograms for dyad **9**. An endothermic "subpeak" (i.e., change in the baseline) at 33.5 °C is present. During subsequent heating–cooling cycles at a rate of 10 °C min$^{-1}$, reversibility of the transition was found. Since a main transition peak could not be detected, the transition found in dyad **9** is different from the ones observed in liposomal and synthetic lipid bilayer membranes.[15] Multiscan DSC measurements revealed that the transition at 33.5 °C is recovered when the temperature was cycled back after heating up to 200 °C. On the other hand, ageing of **9** at a temperature down to −10 °C is required to recover the original endothermic peak when the temperature was cycled back from temperatures much above the transition temperature. Collectively, the transition temperature ($T_c$), the transition enthalpy ($\Delta H$), and the transition entropy ($\Delta S$) of **9** are summarized in Table 1.

**Ground-state electronic absorption spectra**: The absorption spectrum of **9** disclose features of both species, namely, the fullerene and the coumarin. The UV/Vis spectra of dyad **9**, precursor **8**, and $C_{60}$, obtained in toluene, are depicted in Figure 2. The spectrum of **8** is characterized by a broad absorption band in the visible region, with a maximum at 431 nm, while intact $C_{60}$ has a characteristic sharp absorption at 330 nm. On the other hand, in the absorption spectrum of dyad **9**, the absorption band due to the fullerene unit appears broadened, while additional changes are observed in the shape and absorption intensity of the coumarin chromophore (i.e., blueshifted at 429 nm). These results indicate not only the successful functionalization of $C_{60}$ with **8**, but also intradyad ground-state electronic interactions between the coumarin chromophore and $C_{60}$.

Table 1. Transition temperature ($T_c$), transition enthalpy ($\Delta H$) and transition entropy ($\Delta S$) of dyad **9**.

| Dyad | $T_c$ [°C] | $\Delta H$ [kJ mol$^{-1}$] | $\Delta S$ [J mol$^{-1}$ K$^{-1}$] |
|---|---|---|---|
| **9** | 33.5 | 33.9 | 12.6 |

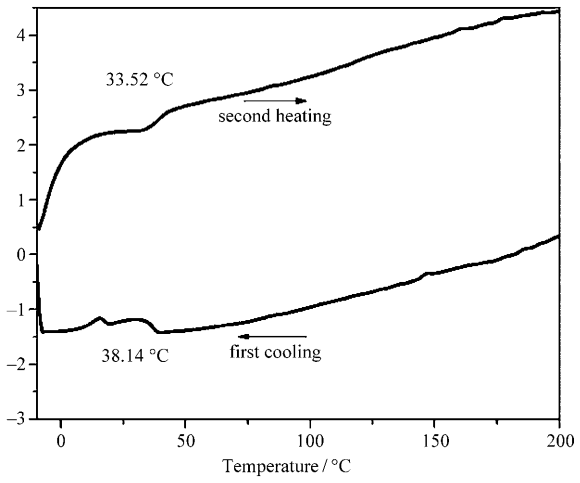


Figure 1. Differential scanning calorimetry thermograms of **9**.

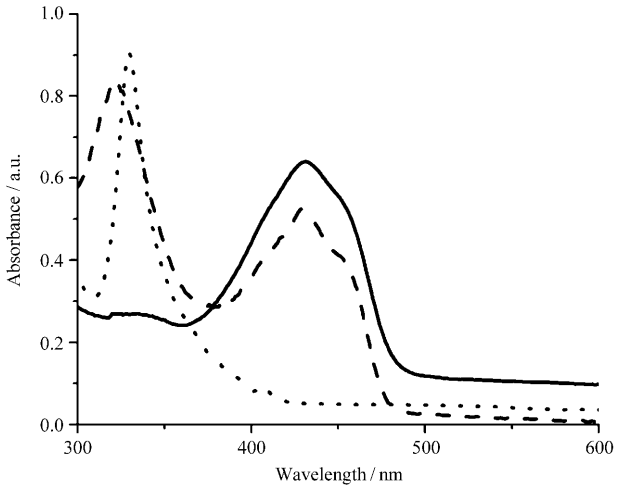


Figure 2. Electronic absorption spectra of **9** (black line), **8** (dashed line), and $C_{60}$ (dotted line), obtained in toluene.

  

**Excited-state fluorescence emission spectra**: Meaningful insight into the excited-state interactions between the photo- and redox-active units in **9**, arose from fluorescence emission measurements. In Figure 3, the steady-state emission spectra of dyad **9** and precursor **8** are compared when excited at 430 nm in toluene. In the spectrum of **9**, the coumarin emission band, with a maximum at 478 nm and a shoulder at 501 nm, is 98% quenched by the $C_{60}$ unit, relative to that of the reference coumarin malonate **8** (the spectra obtained with matching absorbances at the excitation wavelength). Moreover, the coumarin emission maxima in dyad **9** are blueshifted by 10 and 7 nm, respectively, compared with those of the reference compound **8**, mirroring the bathochromic shifts observed in the UV/Vis spectra. It should be noted that the characteristic fluorescence emission of $C_{60}$ at 710 nm is masked by the strong emission of the coumarin unit due to the low quantum yield of $C_{60}$ ($\Phi_{C60}=6\times10^{-4}$).[16] Collectively, these observations suggest efficient quenching of the singlet excited state of the coumarin moiety by the appended fullerene sphere. Changing the solvent from nonpolar toluene to polar THF or dichloromethane, similar fluorescence emission spectral changes for dyad **9**, however, with enhanced fluorescence quenching, were observed. This is attributed to the better solvation the radical ion pairs experience in the polar environment of THF or dichloromethane than in toluene, resulting in lower energies of the developing charge-separated states. From this solvent dependence, efficient electron-transfer quenching the excited singlet state of the coumarin moiety by $C_{60}$ is inferred.

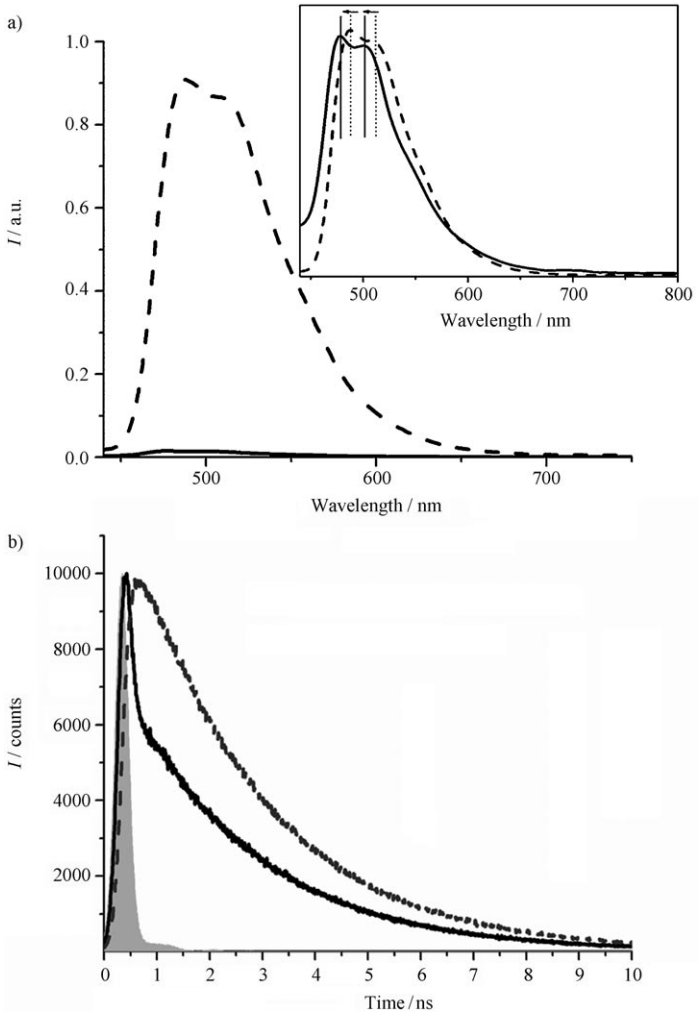


Figure 3. a) Steady-state fluorescence spectra of **9** (black line) compared with **8** (dashed line). Inset: Magnified emission spectra of **9**, showing 1) hypsochromic shift in the emission band of its coumarin chromophore (black line) compared with the precursor **8** (dashed line), and 2) the emission of $C_{60}$ at 710 nm (black line). Measurements performed in toluene at $\lambda_{exc}=430$ nm. b) Fluorescence lifetime decay of **9** (black line) compared with **8** (gray line). Measurements performed at room temperature in toluene at $\lambda_{exc}=430$ nm and $\lambda_{em}=492$ nm.

To probe the photophysical dynamics of the singlet excited state of coumarin in dyad **9**, time-resolved fluorescence emission studies were performed by the time-correlated single photon counting (TCSPC) method. Time-resolved fluorescence decay profiles of coumarin in the absence, reference compound **8**, and presence of $C_{60}$, dyad **9**, are shown in Figure 3b. The fluorescence decay of $^1$coumarin* in **8** either in nonpolar toluene or polar solvents, such as THF and dichloromethane, is exclusively monoexponentially fitted with a lifetime of 2.43 ns. On the other hand, upon photoexcitation at 441 nm of a toluene solution of dyad **9**, analysis of the time profiles for the decay at 492 nm yielded two exponentially decayed components (i.e., a fast and a slow decay) with lifetimes of 58 ps (94%) and 2.41 ns (6%). It should be mentioned that the lifetime of about 58 ps is only an upper limit of the actual lifetime due to the time-resolution limitation our instrument (i.e., 50 ps). Therefore, the fast-decay in dyad **9**, with a lifetime almost 50 times shorter than that of **8**, is attributed to the singlet excited state of coumarin ($^1$coumarin*). This is consistent with what was observed in the steady-state fluorescence emission measurements, in which strong quenching of coumarin due to $C_{60}$ in dyad **9** was observed (see above and Figure 3a). Then, by attributing the fast-decaying component to the charge separation in **9**, the rate constant for charge separation ($k_{CS}$) was determined to be $1.7\times10^{10}$, according to Equation (1). Additionally, the quantum yield $\Phi_{CS}$ for charge separation was calculated to be 0.98, according to Equation (2):

$$k_{CS} = (1/\tau_f)-(1/\tau_0) \quad (1)$$

$$\Phi_{CS} = [(1/\tau_f)-(1/\tau_0)]/(1/\tau_f) \quad (2)$$

in which $\tau_f$ refers to the lifetime of the faster-decaying component in the biexponential fitting function and $\tau_0$ refers to the coumarin fluorescence lifetime.

Time-resolved fluorescence studies performed in polar THF and dichloromethane solvents gave similar results. All photophysical data are collected and presented in Table 2.

**Electrochemistry**: The determination of the redox potentials of **9** is important for the evaluation of the energetics of the

  

Table 2. Fluorescence decay lifetime data for dyad **8** and **9**.

| Solvent | Material | $\tau_f$ [ps] | $k_{CS}$ | $\Phi_{CS}$ |
|---|---|---|---|---|
| $CH_2Cl_2$ | **8** | 2680 | | |
| | **9** | 51 (84%) 2600 (16%) | $1.9\times10^{10}$ | 0.97 |
| THF | **8** | 2630 | | |
| | **9** | 48 (88%) 2570 (12%) | $2.1\times10^{10}$ | 0.99 |
| toluene | **8** | 2430 | | |
| | **9** | 58 (94%) 2410 (6%) | $1.7\times10^{10}$ | 0.98 |

electron-transfer processes. In this direction, to enlighten the intramolecular interaction between the coumarin moiety and $C_{60}$, the electrochemical properties of $C_{60}$, derivative **8**, and dyad **9** were investigated by differential pulse voltammetry (DPV) as well as cyclic voltammetry (CV). The measurements were performed in a mixture of *ortho*-dichlorobenzene (ODCB)/acetonitrile 5:1, with tetrabutylammonium hexafluorophosphate ($TBAPF_6$) as the electrolyte in a standard three-electrode cell with platinum as the working and counter electrode. As shown in Figure 4, DPV and CV measurements revealed that **9** undergoes three reversible one-electron reduction and a one-electron oxidation processes. Comparison of the redox data of $C_{60}$ and **8** with those of **9** indicate that the two reductions of dyad **9** at $-0.91$ and $-1.26$ V are due to the presence of $C_{60}$, while the reduction of coumarin moiety at $-1.82$ V is overlapping with the third reduction peak of $C_{60}$ at $-1.75$ V. On the other hand, the oxidation process at 0.94 V, due to the presence of the coumarin moiety, is anodically shifted by 50 mV, compared with the reference compound **8**. The small cathodic shift observed for the reduction potential of dyad **9** relative to $C_{60}$ is rationalized in terms of the decreased electron affinity monosubstituted fullerenes show relative to intact $C_{60}$.

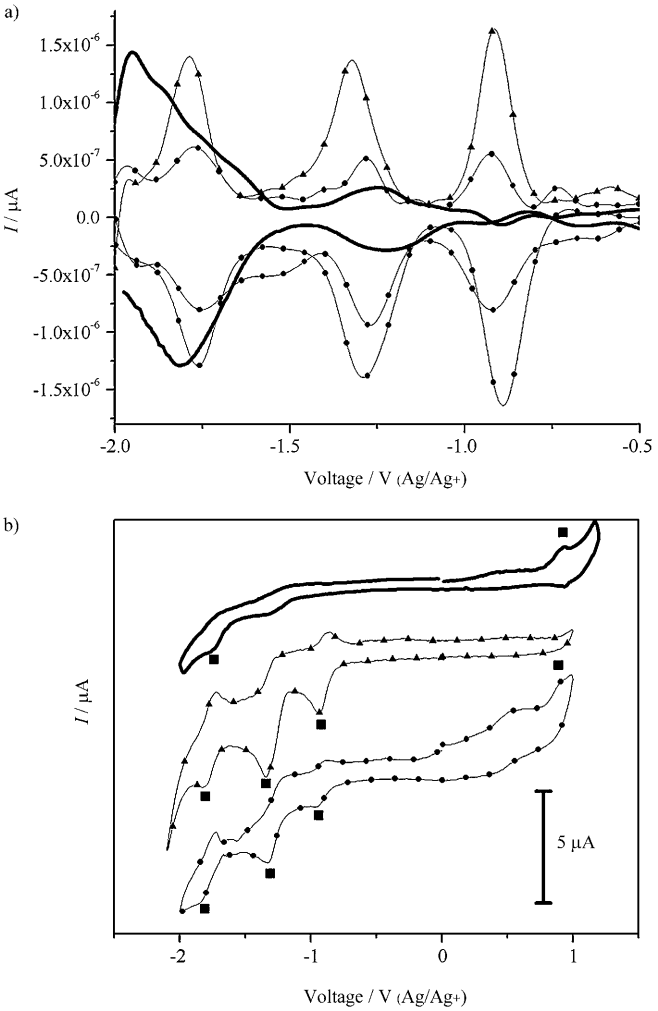


Figure 4. a) Differential pulsed voltammograms (scan rate 20 mV s$^{-1}$) of the $C_{60}$–coumarin dyad **9** (●) as compared with pristine $C_{60}$ (▲) and the coumarin malonate derivative **8** (black), and b) cyclic voltammogram (scan rate 100 mV s$^{-1}$) of the $C_{60}$–coumarin dyad **9** (●) as compared with pristine $C_{60}$ (▲) and the coumarin derivative **8** (black). Conditions: ODCB/MeCN 5:1, 0.1 M $nBu_4NPF_6$ as the electrolyte, Pt wires as working and counter electrodes, and $Ag/AgNO_3$ as reference electrode.

**Ion-binding studies**: To explore the ability of **9** to bind to metals, it was necessary to unmask the methyl ester groups and liberate the carboxylate anions. Treatment of dyad **9** with *t*BuOK/DMSO[8f] quantitatively gave probe **10**, as described in Scheme 3.

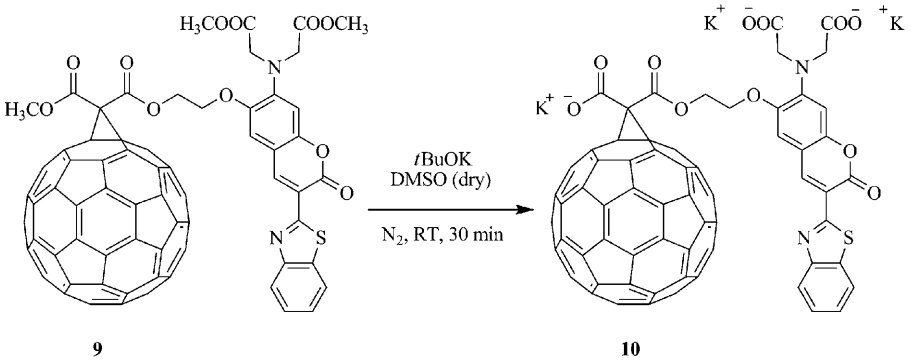


**9** **10**

Scheme 3. Deprotection of **9** to give **10**.

As expected,[8g] probe **10** exhibited moderate affinity to $Zn^{2+}$ ions in contrast to a far stronger interaction with $Pb^{2+}$. We therefore studied the fluorescence profile of **10** in solutions of increasing $Pb^{2+}$ concentrations, as shown in Figure 5. The ion-free fullerene–coumarin probe **10** exhibits an excitation maximum at 470 nm, which shifts to 468 nm upon $Pb^{2+}$ binding. When excited, the ion-free form of **10** shows an emission maximum at 503 nm, which shifts to 500 nm upon $Pb^{2+}$ binding with a small decrease in fluorescence intensity at $Pb^{2+}$ saturation levels. The dissociation constant of probe **10** was calculated according to Tsien's algorithm[17] as 72 μM.

  

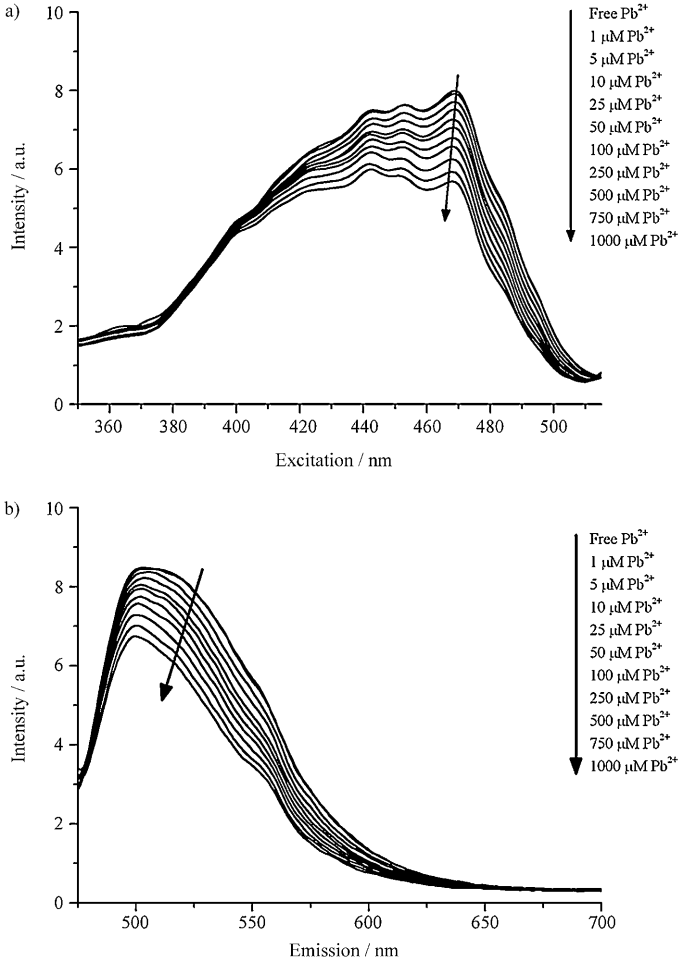


Figure 5. a) Excitation and b) emission spectra of **10** in solutions of increasing $Pb^{2+}$ concentrations in nanopure water. The excitation wavelength was set at 470 nm.

The potential use of dyad **10** as a $Pb^{2+}$ probe in biological or environmental systems is shown in an ion competition study of a range of metals. Materials were excited at the isosbestic point (400 nm) and 470 nm, and the fluorescence intensity ratio was calculated (Figure 6). Given that addition of $Pb^{2+}$ results in a decrease of fluorescence intensity when the system is excited at 470 nm, the fluorescence ratio $F_{400}/F_{470}$ is expressed in positive numbers. In the first set of measurements, the fluorescence ratio after addition of 50 μM $Pb^{2+}$ is shown (black bar) and compared with that of 50 μM of the free dye (gray bar). The rest of the measurement sets indicate a fluorescence ratio of the dye in the presence of one equivalent of metal (gray bars) versus the fluorescence ratio after addition of one equivalent of $Pb^{2+}$ to the same sample (black bars). Binding by these metal ions appears to be weak, since subsequent addition of $Pb^{2+}$ to these solutions increases the fluorescence ratio of the dye–metal solution to the same extent as in the case of the first measurement (competitive ion-free solution).

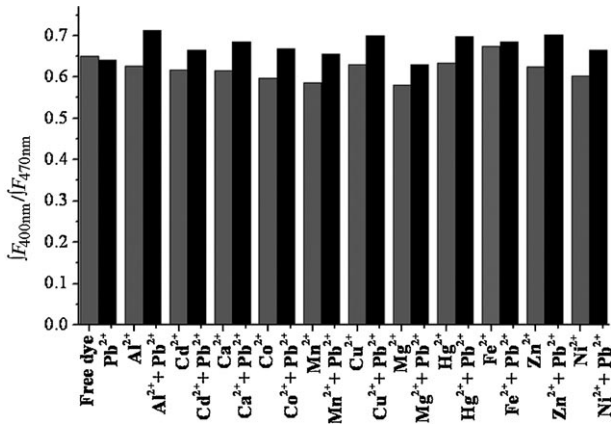


Figure 6. Ion competition study of **10**.

## Conclusion

The preparation of **9** has been carried out by following the established cyclopropanation Bingel protocol via suitably functionalized coumarin–malonate **8**. The electronic properties of the newly synthesized dyad **9** were probed by electronic absorption and fluorescence spectroscopy, which suggest the existence of electronic interactions between the fullerene and the coumarin of the dyad, in the ground and the excited states. The characteristic emission of coumarin was quenched in dyad **9** following intramolecular electron transfer, from the coumarin to $C_{60}$, as inferred by photoluminescence experiments performed in apolar and polar solvents. Time-resolved fluorescence measurements revealed lifetimes for the **9** at a maximum of 50 ps, while the quantum yield reached unity. Moreover, electrochemistry revealed the redox potentials of dyad **9**, where a cathodic shift observed for the reduction potential of **9** compared with intact $C_{60}$. Lastly, the methyl esters in dyad **9** have been cleaved to liberate free carboxylate moieties in dyad **10**. The latter was tested for binding divalent metal cations, while ion competition studies demonstrated that probe **10** is selective for $Pb^{2+}$ complexation. Thus, such $C_{60}$–coumarin dyads may find interesting applications as selective artificial receptors in a wide range of biological, environmental, and chemical processes.

## Experimental Section

**General**: All chemicals were purchased from chemical suppliers and used without further purification. Dry solvents were prepared by using customary literature procedures.[18] TLC: Riedel-de Haën silica gel F254. Detection: UV lamp and iodine chamber. Flash chromatography (FC): Aldrich silica gel 60 (230–400 mesh, 0.04–0.063 nm). NMR spectra were recorded on a Bruker AC 300 FT-NMR spectrometer; the chemical shifts are given in parts per million relative to tetramethylsilane. Differential scanning calorimetry (DSC) measurements were performed on a Q 200 differential scanning calorimeter from TA Instruments. In a typical experiment, the sample was placed in hermetically closed aluminum pan under helium flow. Standard DSC heating and cooling scans were performed at 10 °C min$^{-1}$. Electrochemistry studies were performed by using a standard three-electrode cell. Platinum wires were used as counter and

  

working electrodes. Silver/silver nitrate ($Ag/AgNO_3$ 0.1 M in acetonitrile) was used as a reference electrode. $TBAPF_6$ (98%) was used as the electrolyte and was recrystallized three times from acetone and dried in a vacuum at 100°C. Before each experiment the cell was purged with high purity $N_2$ for 5 min. Before the start of the measurement the inert gas was turned to "blanket mode". Measurements were recorded by using an EG&G Princeton Applied Research potensiostat/galvanostat Model 2273 connected to a personal computer running PowerSuite software. The working electrode was cleaned before each experiment through polishing using a cloth and 6, 3, and 1 μm diamond pastes. The $Ag/AgNO_3$ electrode was calibrated before each experiment by running cyclic voltammetry on ferrocene. .Mass spectra were recorded on a MALDI-TOF mass spectrometer. UV/Vis spectra were recorded on a Perkin–Elmer UV/VIS/NIR spectrometer Lamda 19. Mid-IR spectra in the region 550–4000 $cm^{-1}$ were obtained on a Fourier-transform IR spectrometer (Equinox 55 from Bruker Optics) equipped with a single reflection diamond ATR accessory (DuraSamp1IR II by SensIR Technologies). A drop of the solution was placed on the diamond surface, followed by evaporation of the solvent, in a stream of nitrogen, before recording the spectrum. Typically, 100 scans were acquired at 4 $cm^{-1}$ resolution. Fluorescence spectra were taken on an Aminco Bowman spectrofluorimetre (Spectronocs Co., USA) and a Fluorolog-3 Jobin Yvon-Spex spectrofluorometer (model GL3–21). Picosecond time-resolved fluorescence spectra were measured by the time-correlated single-photon counting (TCSPC) method on a NanoLog spectrofluorometer (Horiba Jobin Yvon), using a laser diode as an excitation source (NanoLED, 441 nm, 200 ps pulse width). Lifetimes were evaluated with the DAS6 Fluorescence-Decay Analysis Software. All measurements were performed at room temperature.

**Preparation of 2**: $K_2CO_3$ (415 mg, 3 mmol) was added to a suspension of **1**[13] (7350 mg, 3 mmol) in anhydrous DMF (60 mL). After 20 min, benzyl 2-bromomethyl ether (935 mg, 4.3 mmol, 688 μL) was added to the reaction mixture. After heating the suspension for 14 h at 110°C under nitrogen, the reaction was complete. The system was cooled to room temperature, dissolved in $H_2O$, and extracted with ethyl acetate. The organic phase was dried over $Na_2SO_4$, filtered, and then the solvent was evaporated to dryness in vacuum, yielding a yellow solid (1.055 g, 92%). UV/Vis ($CH_2Cl_2$): $\lambda$ = 358, 260 nm; ATR-IR: $\tilde{\nu}$ = 3085–2850, 1525, 1496 $cm^{-1}$; $^1H$ NMR (300 MHz, $CDCl_3$): $\delta$ = 3.86 (t, $J_1$ = 4.5 Hz, 2H), 4.24 (t, $J_1$ = 4.5 Hz, 2H), 4.65 (s, 2H), 5.05 (s, 2H), 7.07 (s, 1H), 7.13 (d, $J$ = 3 Hz, 1H), 7.36–7.42 (m, 10H), 7.48 ppm (d, $J$ = 3 Hz, 1H); $^{13}C$ NMR (300 MHz, $CDCl_3$) $\delta$ = 64.9, 68.2, 69.8, 72.9, 110.9, 117.1, 121.4, 127.6 (2C), 127.7 (2C), 128.3, 128.4 (3C), 128.7 (2C), 137.6, 137.9, 140.0, 146.7, 152.1 ppm; MALDI-TOF-MS (dithranol as matrix): $m/z$: 379 [$M^+$].

**Preparation of 3**: Powdered 10% Pt/C (10 mg) was added to a solution of **2** (1.040 g, 2.8 mmol) in dry ethanol under an $N_2$ atmosphere at room temperature. Removal of $N_2$ in vacuo followed by addition of $H_2$ and stirring of the reaction mixture for 17 h led to the formation of the product. The reaction was monitored by TLC (ethyl acetate/petroleum ether 30/70). The solution was filtered and the solvent was removed under reduced pressure. The remained residue was further purified via column chromatography (silica gel, ethyl acetate/petroleum ether 20/80) to give **3** (800 mg, 80%). UV/Vis ($CH_2Cl_2$): $\lambda$ = 366, 304, 251 nm; ATR-IR: 3475, 3370, 3085–2860, 1617, 1509, 1452 $cm^{-1}$; $^1H$ NMR (300 MHz, $CDCl_3$): $\delta$ = 3.82 (t, $J_1$ = 4.5 Hz, 2H), 4.13 (t, $J_1$ = 4.5 Hz, 2H), 4.64 (s, 2H), 5.00 (s, 2H), 6.32(dd, $J_1$ = 9 Hz, $J_2$ = 3 Hz, 1H) 6.43 (d, $J$ = 2.7 Hz, 1H), 6.76(d, $J$ = 9 Hz, 1H), 7.33–7.45 ppm (m, 10H); $^{13}C$ NMR (300 MHz, $CDCl_3$): $\delta$ = 68.4, 69.0, 69.8, 72.8, 102.4, 102.7, 114.2, 127.1 (2C), 127.45 (3C), 127.40, 128.18(2C), 128.12 (2C), 137.2, 137.8, 138.2, 140.5, 153.9; MALDI-TOF MS (dithranol as matrix): $m/z$: 349 [$M^+$].

**Preparation of 4**: This compound was prepared by following a previously published procedure[13] using **3** (0.500 g, 1.43 mmol), *tert*-butyl bromoacetate (0.875 g, 5.72 mmol), diisopropylethylamine (0.740 g, 5.72 mmol), and sodium iodide (0.215 g, 1.43 mmol) in DMF (5 mL) as the solvent to give the product after workup and purification (0.215 g, 30%). UV/Vis ($CH_2Cl_2$): $\lambda$ = 362, 300, 250 nm; ATR-IR: 3085–2850, 1745, 1606, 1506, 1454 $cm^{-1}$; $^1H$ NMR (500 MHz, $CDCl_3$): $\delta$ = 3.72 (s, 6H), 3.82 (t, $J_1$ = 4.5 Hz, $J_2$ = 5 Hz, 2H), 4.16 (t, $J_1$ = 5.5 Hz, $J_2$ = 4.5 Hz, 2H), 4.25 (s, 4H), 4.65 (s, 2H), 5.02 (s, 2H), 6.54 (dd, $J_1$ = 8.7 Hz, $J_2$ = 3.5 Hz, 1H), 6.59 (d, $J_1$ = 2.5 Hz, 1H), 6.83 (d, $J_1$ = 9 Hz, 1H),7.47–7.34 ppm (m, 10H); $^{13}C$ NMR (500 MHz, $CDCl_3$): $\delta$ = 51.4 (2C), 53.1 (2C), 68.4, 68.7, 70.1, 72.9, 106.4, 107.1, 115.2, 127.3 (2C), 127.4 (3C), 127.6, 128.1 (3C), 128.2, 137.0, 137.9, 140.1, 144.6, 153.5, 171.4 ppm (2C); MALDI-TOF MS (dithranol as matrix): $m/z$: 493 [$M^+$].

**Preparation of 5**: This compound was prepared according to a previously described method[13] using **4** (0.215 g, 0.45 mmol) and phosphoryl chloride (0.064 mL, 0.70 mmol) in DMF (5 mL) to give the product after workup and purification (0.175 g, 72%). UV/Vis ($CH_2Cl_2$): $\lambda$ = 325, 292, 251 nm; ATR-IR: 3085–2850, 1745, 1664, 1600, 1517 $cm^{-1}$; $^1H$ NMR (500 MHz, $CDCl_3$): $\delta$ = 3.67 (s, 6H), 3.71 (t, $J_1$ = 3 Hz, $J_2$ = 8 Hz, 2H), 4.09 (t, $J_1$ = 3 Hz, $J_2$ = 8 Hz, 2H), 4.18 (s, 4H), 4.53 (s, 2H), 5.07 (s, 2H), 6.24 (s, 1H), 7.36–7.28 (m, 11H), 10.27 ppm (s, 1H); $^{13}C$ NMR (500 MHz, $CDCl_3$): $\delta$ = 51.9, 53.8, 68.1, 68.3, 71.1, 73.0, 102.5, 111.3, 117.9, 127.2 (2C), 127.56 (2C), 127.59, 128.1, 128.3 (2C), 128.6 (2C), 136.3, 137.9, 143.8, 146.1, 157.3, 171.0 (2C), 187.5; MALDI-TOF MS (dithranol as matrix): $m/z$: 521 [$M^+$].

**Preparation of 6**: This compound was prepared according to a previously described method[13] using compound **5** ( 0.175 g, 0.33 mmol), 10% Pd/C (0.02 g) as the hydrogenation catalyst and ethyl acetate (10 mL) as the solvent to give the product after workup and purification (0.112 g, 98%). UV/Vis ($CH_2Cl_2$): $\lambda$ = 357, 309, 255 nm; ATR-IR (): 3454, 2950–2850, 1735, 1629, 1575, 1510 $cm^{-1}$; $^1H$ NMR (300 MHz, $CDCl_3$): $\delta$ = 3.71 (t, $J_1$ = 3 Hz, $J_2$ = 4.8 Hz, 2H), 3.80 (s, 6H), 4.04 (t, $J_1$ = 3 Hz, $J_2$ = 4.8 Hz, 2H), 4.20 (s, 4H), 6.13 (s1H), 6.85 (s, 1H), 9.57 (s, 1H), 11.17 ppm (s, 1H); $^{13}C$ NMR (300 MHz, $CDCl_3$): $\delta$ = 51.9, 52.4, 53.8, 54.1, 71.7, 72.8, 104.2, 107.2, 113.2, 115.6, 117.9, 118.4, 171.5, 172.3, 193.2 ppm; MALDI-TOF MS (dithranol as matrix): $m/z$: 341 [$M^+$].

**Preparation of 7**: Compound **6** (0.112 mg, 0.33 mmol) was added to a solution of methyl α-benzothiazolyl acetate[14] (0.07 g, 0.33 mmol) and piperidine(0.028 g, 0.33 mmol) in dry methanol (3 mL) and the yellow/orange suspension was heated to 70°C for 1 h. The system was then cooled to 0°C and the precipitated yellow solid filtered by suction and washed with diethyl ether to give the product (0.139 g, 85%). UV/Vis ($CH_2Cl_2$): $\lambda$ = 433 nm; ATR-IR: 3400–3165, 2950–2850, 1737, 1708, 1617, 1550, 1510, 1411, 1230–1163 $cm^{-1}$; $^1H$ NMR (300 MHz, $CDCl_3$): $\delta$ = 3.72 (s, 2H), 3.84 (s, 6H) 4.09 (s,2H), 4.24 (s, 4H), 6.64 (s, 1H), 6.98 (s, 1H), 7.39(t, $J$=5.2 Hz, 1H), 7.50 (t, $J$ = 5.2 Hz, 1H), 7.60 (d, $J$ = 7.8 Hz, 1H), 8.03 (d, $J$ = 8.1 Hz, 1H), 8.92 ppm (s, 1H); $^{13}C$ NMR (300 MHz, $CDCl_3$): $\delta$ = 52.5 (2C), 54.2 (2C), 60.8, 61.0, 104.1, 110.5, 112.1, 116.4, 121.6, 122.4, 124.9, 126.3, 136.5, 141.1, 145.0, 147.2, 150.5, 152.4, 160.4, 160.7, 171.6 ppm (2C); MALDI-TOF MS (dithranol as matrix): $m/z$: 498 [$M^+$].

**Preparation of 8**: Pyridine (0.137 mg, 1.74 mmol) was added to a solution of coumarin dye **7** (0.038 m, 0.076 mmol) in dry $CH_2Cl_2$ (4 mL), under an $N_2$ atmosphere. After stirring at room temperature for 10 min, the mixture was cooled to 0°C and a solution of methyl malonyl chloride (0.023 g, 0.168 mmol) in dry $CH_2Cl_2$ (2 mL) was added dropwise. The reaction mixture was stirred at room temperature for 24 h and monitored by TLC (ethyl acetate/petroleum ether 50/50). At the end of the reaction, the solvent was removed under reduced pressure and the residue was further purified by column chromatography (silica gel, ethyl acetate/petroleum ether 70/20) to afford the product (0.036 mg, 79%). UV/Vis ($CH_2Cl_2$): $\lambda$ = 430 nm; ATR-IR: 3400–3165, 2950–2850, 1745, 1730, 1705, 1614, 1550, 1510, 1411, 1240, 1207–1150 $cm^{-1}$; $^1H$ NMR (300 MHz, $CDCl_3$): $\delta$ = 3.48 (s, 2H), 3.79 (s, 3H) 3.80 (s, 6H), 4.24 (dd, $J_1$ = $J_2$ = 4.5 Hz, 2H), 4.26 (s, 4H), 4.46 (dd, $J_1$ = $J_2$ = 4.5 Hz, 2H), 6.66 (s, 1H), 7.00 (s, 1H), 7.40 (t, $J$ = 7.2 Hz, 1H), 7.51 (t, $J$ = 7.8 Hz, 1H), 7.96 (d, $J$ = 8.1 Hz, 1H), 8.05 (d, $J$ = 8.4 Hz, 1H), 8.96 ppm (s, 1H); $^{13}C$ NMR (300 MHz, $CDCl_3$): $\delta$ = 41.0, 52.3 (2C), 52.6, 53.8 (2C), 63.3, 66.9, 104.1, 110.7, 111.8, 116.3, 121.7, 122.5, 124.9, 126.3, 136.5, 141.1, 144.9, 146.6, 150.7, 152.4, 160.4, 160.7, 166.5, 166.7, 170.7 (2C); MALDI-TOF MS (dithranol as matrix): $m/z$: 598 [$M^+$].

**Preparation of 9**: DBU (0.005 g, 0.035 mmol) was added dropwise to a suspension containing $C_{60}$ (0.025 g 0.034 mmol), $CBr_4$ (0.010 g 0.030 mmol), and **8** (0.016 g, 0.026 mmol) in dry toluene (100 mL) under $N_2$ atmosphere. The reaction mixture was stirred at room temperature for 24 h, and the progress of the reaction was monitored by TLC (ethyl

  

acetate/toluene 30/70). The product was isolated by flash chromatography (silica gel, toluene) and dried in vacuo to give the product (0.007 g, 19%). UV/Vis ($CH_2Cl_2$): $\lambda = 429$ nm; ATR-IR: 2950–2850, 1739, 1705, 1610, 1550, 1512, 1456, 1267, 1236–1163 $cm^{-1}$. $^1H$ NMR (300 MHz, $CDCl_3$): $\delta = 3.85$ (s, 6H), 4.07 (s, 3H), 4.27 (s, 4H), 4.41 (dd, 2H), 4.83 (dd, 2H), 6.90 (s, 1H), 7.09 (s, 1H), 7.44 (t, 1H), 7.56 (t, 1H), 7.96 (d, 1H), 8.15 (d, 1H), 9.28 ppm (s, 1H); MALDI-TOF MS (dithranol as matrix): $m/z$: 1316 [$M^+$].

## Acknowledgements

Partial financial support from the EU FP7, Capacities Program, NANOHOST project (GA 201729) to N.T. is acknowledged. N.T. also thanks COST network MP0901 NanoTP for support.

[1] a) *Fullerenes: Principle and Applications* (Eds.: F. Langa, J. F. Nierengarten), RSC, Cambridge, **2007**; b) J. F. Nierengarten, *New J. Chem.* **2004**, *28*, 1177–1191; c) N. Martin, L. Sanchez, M. A. Herranz, B. Illescas, D. M. Guldi, *Acc. Chem. Res.* **2007**, *40*, 1015–1024; d) N. Martin, *Chem. Commun.* **2006**, 2093–2104.
[2] D. M. Guldi, *Chem. Commun.* **2000**, 321–327.
[3] J. M. Tour, *Acc. Chem. Res.* **2000**, *33*, 791–804.
[4] *Fullerenes: From Synthesis to Optoelectronic Properties* (Eds.: D. M. Guldi, N. Martin), Kluwer Academic Publishers, Dordrecht, **2002**.
[5] R. Kiebooms, R. Menon, K. Lee in *Handbook of Advanced Electronic and Photonic Materials and Devices* (Ed.: H. S. Nalwa), Academic Press, San Diego, **2001**.
[6] a) S. G. Liu, L. Echegoyen, *Eur. J. Org. Chem.* **2000**, 1157–1163; b) J. Bourgeois, P. Seiler, M. Fibbioli, E. Pretsch, F. Diederich, L. Echegoyen, *Helv. Chim. Acta* **1999**, *82*, 1572–1652; c) A. Kumar, S. K. Menon, *Supramol. Chem.* **2010**, *22*, 46–56.
[7] H. E. Katerinopoulos, *Curr. Pharm. Des.* **2004**, *10*, 3835.
[8] a) K. Komatsu, Y. Urano, H. Kojima, T. Nagano, *J. Am. Chem. Soc.* **2007**, *129*, 13447–13454; b) D. Citterio, J. Takeda, M. Kosugi, H. Hisamoto, S.-I. Sasaki, H. Komatsu, K. Suzuki, *Anal. Chem.* **2007**, *79*, 1237–1242; c) M. A. Haidekker, T. P. Brady, D. Lichlyter, E. A. Theodorakis, *J. Am. Chem. Soc.* **2006**, *128*, 398–399; d) M. Suresh, A. Das, *Tetrahedron Lett.* **2009**, *50*, 5808–5812; e) F. Liepouri, T. G. Deligeorgiev, Z. Veneti, C. Savakis, H. E. Katerinopoulos, *Cell Calcium* **2002**, *31*, 221–227; f) E. Roussakis, F. Liepouri, A.-P. Nifli, E. Castanas, T. G. Deligeorgiev, H. E. Katerinopoulos, *Cell Calcium* **2006**, *39*, 3–11; g) E. Roussakis, S. A. Pergantis, H. E. Katerinopoulos, *Chem. Commun.* **2008**, 6221–6223; h) E. Roussakis, S. Voutsadaki, E. Pinakoulaki, D. P. Sideris, K. Tokatlidis, H. E. Katerinopoulos, *Cell Calcium* **2008**, *44*, 270–275.
[9] a) Z. S. Wang, Y. Cui, K. Hara, Y. Dan-oh, C. Kasada, A. Shinpo, *Adv. Mater.* **2007**, *19*, 1138–1141; b) J. H. Jou, Y. S. Chiu, R. Y. Wang, H. C. Hu, C. P. Wang, H. W. Lin, *Org. Electron.* **2006**, *7*, 8–15; c) S. Sarkar, R. Pramanik, D. Seth, P. Setua, N. Sarkar, *Chem. Phys. Lett.* **2007**, *433–449*, 102–108; d) N. Koumura, Z.-S. Wang, S. Mori, M. Miyashita, E. Suzuki, K. Hara, *J. Am. Chem. Soc.* **2006**, *128*, 14256–14257; e) B. M. Wong, J. G. Cordaro, *J. Chem. Phys.* **2008**, *129*, 214703.
[10] a) S. Nascimento, M. J. Brites, C. Santos, B. Gigante, A. Fedorov, M. N. Berberan-Santos, *J. Fluoresc.* **2006**, *16*, 245–250; b) M. Joao Brites, C. Santos, S. Nascimento, B. Gigantea, M. N. Berberan-Santos, *Tetrahedron Lett.* **2004**, *45*, 6927–6930.
[11] a) C. Bingel, *Chem. Ber.* **1993**, *126*, 1957; b) X. Camps, A. Hirsch, *J. Chem. Soc. Perkin Trans. 1* **1997**, 1595–1596.
[12] a) Y. Nakamura, M. Suzuki, Y. Imai, J. Nishimura, *Org. Lett.* **2004**, *6*, 2797–2799; b) G. E. Ball, G. A. Burley, L. Chaker, B. C. Hawkins, J. R. Williams, P. A. Keller, S. G. Pyne, *J. Org. Chem.* **2005**, *70*, 8572–8574; c) K. S. Coleman, S. R. Bailey, S. Fogden, M. L. H. Green, *J. Am. Chem. Soc.* **2003**, *125*, 8722–8723; d) T. Umeyama, N. Tezuka, M. Fujita, Y. Matano, N. Takeda, K. Murakoshi, K. Yoshida, S. Isoda, H. Imahori, *J. Phys. Chem. C* **2007**, *111*, 9734–9741; e) S. P. Economopoulos, G. Pagona, M. Yudasaka, S. Iisima, N. Tagmatarchis, *J. Mater. Chem.* **2009**, *19*, 7326–7331.
[13] F. Liepouri, E. Foukaraki, T. G. Deligeorgiev, H. E. Katerinopoulos, *Cell Calcium* **2001**, *30*, 331.
[14] H. Iatridou, E. Foukaraki, M. A. Kuhn, E. M. Marcus, R. P. Haugland, H. E. Katerinopoulos, *Cell Calcium* **1994**, *15*, 190.
[15] a) D. Chapman, *Biomembrane and Functions*, VCH, Weinheim, **1984**; b) Y. Okahata, R. Ando, T. Kunitake, *Ber. Bunsen-Ges.* **1981**, *85*, 789.
[16] C. S. Foote, *Top. Curr. Chem.* **1994**, *169*, 347–363.
[17] G. Grynkiewicz, M. Poenie, M. Y. Tsien, *J. Biol. Chem.* **1985**, *260*, 3440–3450.
[18] D. D. Perrin, W. L. F. Amarego in *Purification of Laboratory Chemicals*, 3rd ed., Pergamon, Oxford, **1988**.

Received: June 11, 2010
Published online: September 10, 2010

  